System and method for flight envelope expansion via piezoelectric actuation

Ioan Ursu
INCAS – National Institute for Aerospace Research "Elie Carafoli"
Senior Researcher
Iuliu Maniu 220, Bucharest 061126, Romania

Dragos Daniel Ion Guta
INCAS – National Institute for Aerospace Research "Elie Carafoli"
Senior Researcher

George Tecuceanu
INCAS – National Institute for Aerospace Research "Elie Carafoli"
Senior Researcher

Alexandru-Gabriel Persinaru
INCAS – National Institute for Aerospace Research "Elie Carafoli"
Aerospace Engineer

Daniela Enciu
INCAS – National Institute for Aerospace Research "Elie Carafoli"
Research Scientist
Corresponding author: enciu.daniela@incas.ro

Ionel Popescu
STRAERO – Institute for Theoretical and Experimental Analysis of Aeronautical-Astronautics Structures
Aerospace Engineer

Cornel Stoica
INCAS – National Institute for Aerospace Research "Elie Carafoli"
Senior Researcher

ABSTRACT

The paper presents the design and the complex tests of a laboratory demonstrator which aims to show that it is possible to increase the flutter speed and thus to widen the aircraft flight envelope. The demonstrator was developed within the national UEFISCDI Project "Antiflutter demonstrator with piezoelectric actuation" (AFDPA) and is in fact an intelligent model of wing, which is itself a control system, with sensors, piezo actuator and an implemented control law. Research and tests in the subsonic wind tunnel are underway and will be completed until September this year. The piezoelectric actuator was manufactured and tested. The working of the control law based on the method of receptance was studied by numerical simulations and was verified on a laboratory scale model. The main advantage of the piezo actuator, the bandwidth (about 30 Hz, versus the measured about 5 Hz flutter frequency), is exploited. The main advantage of the receptance method of eigenvalues assignement is that the control law is obtained based on measurements rather than on the conventional matrix theory, which is typically for state space methods. It is important to mention that the receptance method requires the online measurement of frequency response functions so that there is no requirement to know or to evaluate the structural mass, damping and stiffness matrices, or the

aerodynamic matrices. Also, the difficult operations of model order reduction and observer building to estimate the unmeasured state variables are avoided.
The content of the paper refers in detail to technical solutions for wing model design, for amplification of the actuator output displacement, simultaneously with the optimization of useful force, and to preliminary experimental results in subsonic wind tunnel.

KEYWORDS: *active control, flutter frequency, flutter speed, flight envelope, receptance method*

NOMENCLATURE

Latin
AFDPA - Antiflutter demonstrator with piezoelectric actuation
b - influence vector
C - damping matrix
K - stiffness matrix
M - mass matrix
p - external perturbation
t - time
u - control
V - voltage

Greek
δ – deflection angle
τ - delay

1 INTRODUCTION

There is a fairly clear description of "aeroelastic flutter" on Wikipedia: "Flutter is a self-feeding and potentially destructive vibration where aerodynamic forces on an object couple with a structure's natural mode of vibration to produce rapid periodic motion".
In principle, the variation of eigenvalues of a structural model, driven by aerodynamic flow variation is studied in the linear frame. The flow variation causes the change of the aerodynamic forces that are proportional to the flow velocity of air and with the degrees of freedom of the system; in turn, this modifies the eigenvalues of the aeroelastic system until they become "unstable". Flutter occurs when the air speed reaches a speed called the flutter speed.
The purpose of this paper is to present a solution to counteract the flutter, based on the use of an actuator consisting in V-shaped two piezo stacks (see kinematic scheme in Fig. 1). This idea is developed in the AFDPA project [1] and ends as a demonstrator in the wind tunnel.

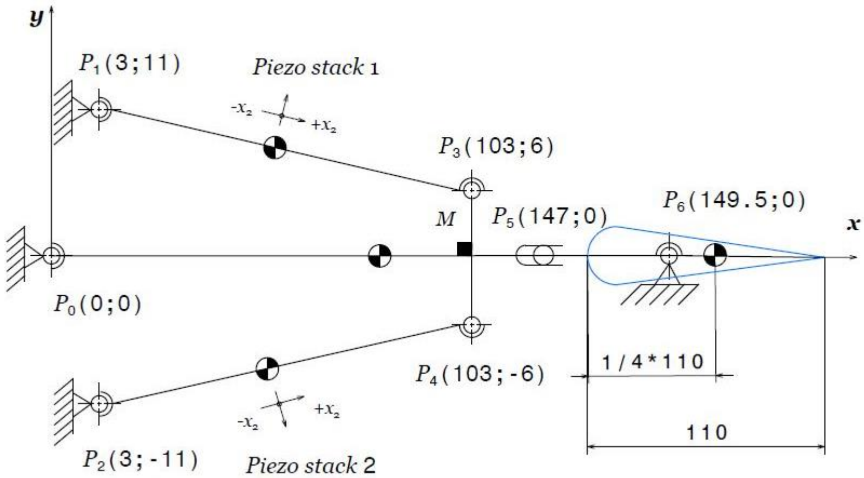

Figure 1: Kinematic scheme of aileron actuation with 2 V-shaped piezo stacks; coordinates in mm

2 DESIGNING AND ACHIEVEMENT OF WING MODEL WITH AILERON

The demonstrator for rising the speed value when the flutter occur in the wind tunnel is represented by a wing made from a spar (longeron) covered by an aerodynamic layer (profile NACA 0012). The wing has a primary flight control surface, an aileron, at one end. At the other end of the longeron there is a flange whose role is to fix the wing in the subsonic tunnel. The spar is a rectangular tube (1200x120x25) with 1 mm thickness and provided with notches to control its stiffness. The elements defining the aerodynamic surface are made from wood or resin ROHACELL 71S. The wing structure is given in Fig. 2.

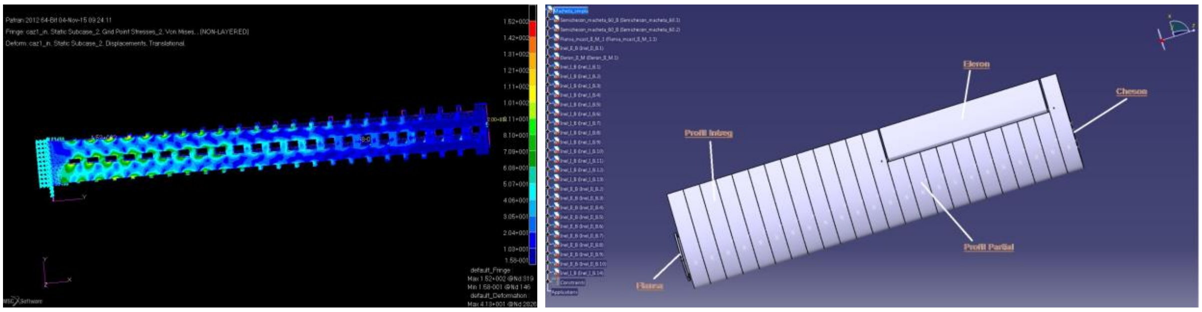

Figure 2 Left: the lonjeron; right: the structure of the wing

3 DESIGNING AND ACHIEVEMENT OF THE PIEZOELECTRIC ACTUATOR

The kinematic scheme of the actuator is represented in Fig. 1. The xOy system of axes is considered. The coordinates are expressed in [mm]. According to the conception and the rigors of actuation of such actuators, the piezo stacks are arranged along the segments P_1P_3 and P_2P_4, respectively. When the stack P_1P_3 is activated by increasing supply voltage V, $V_{01}+\Delta V(t-\tau)$, which determines its extension to move to the right and slightly below the articulated point P_3, the stack P_2P_4 is supplied with the voltage $V_{02}+\Delta V(t-\tau)$

$$\Delta V\left(t-\tau\right)=\begin{cases}0, t\le\tau\\ \Delta V, t>\tau\end{cases} \tag{1}$$

which causes the withdrawal to the left and slightly upward of the articulated point P_4 therefore to not oppose resistance to movement down of the articulated point P_5 in the slider crank mechanism. This provides the movement with positive angle (up) δ of the aileron. The two stacks are successively active versus passive, in the sense of the presented description. The constant τ defines a delay in the application of voltage to "active" stack, to ensure the withdrawal of passive stack. The piezo actuator on the test bench is presented in Fig. 3.

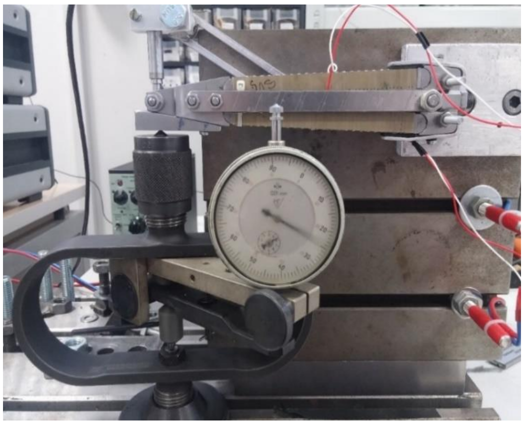
Figure 3: Piezoactuator mounted on the test bench of INCAS Mechatronics Lab

The piezo stacks NAC2022-H98-AO1 were bought from NOLIAC and have the following basic properties: height 98 mm, stroke 148.8 μm, capacitance 19010 nF, maximal force developed 4200 N, maximum operating temperature 150 °C, material NCE51F. The advantage of the piezo actuators is their small size, large bandwidth and, not least, high energy density. There is a disadvantage linked to their lower strokes. It is important to note that, for the antiflutter aero-elastic control to be effective, the deflection of the control surface must be at least 5-6 degrees, to the frequency range of at least 25 to 30 Hz, as it is stated in the paper [9].

Measurements of the displacement-force at the level of point P_5 were performed (Figure 4). The displacement of 650 μm corresponds to a half of sinusoid without load. The double, 1300 μm, is an increase of approximate 10 times of the piezo stack stroke given by the provider, 148.8 μm. The developed maximum force, as measured by loading with resorts becoming increasingly stronger on the other half of the sinusoid, is 230 N. Thus, on the shaft P_1P_3 the force of 4600 N (close to 4200 N given by the provider) is checked. Details are given in [2].

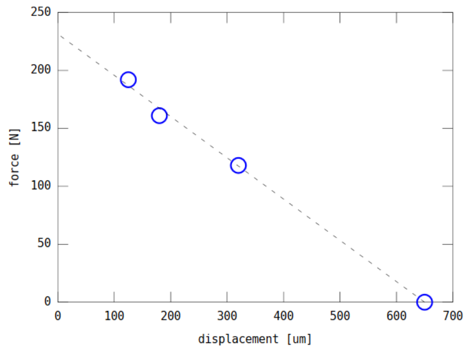

Figure 4: Experimental measurements displacement-force at the level of point P_5

The calculation of the aileron deflection, assuming to neglect the elasticities, the friction and the aerodynamic load on aileron, takes into account the following reasons:

a) simplifying hypothesis: because only one stack is active, consider that the physical model of the actuation is that of Fig. 5, which represents the sequence of the aileron up deflection by activating the piezo stack placed on the segment;

b) the lever P_1P_3 is articulated with the lever P_3M which is solidary linked with the shaft P_0P_5 and in the point P_5 there is a slider crank type joint for aileron actuation;

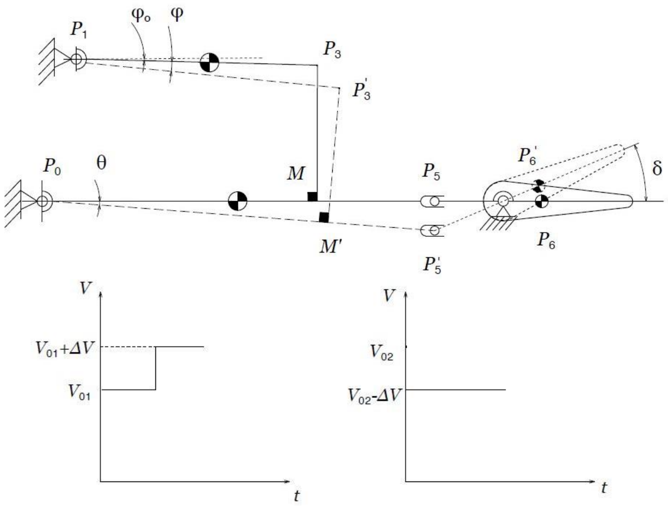

Figure 5: Above: a simple physical model of aileron actuation; below: the form of voltage signals at the inputs of the two piezo stacks, in a time sequence

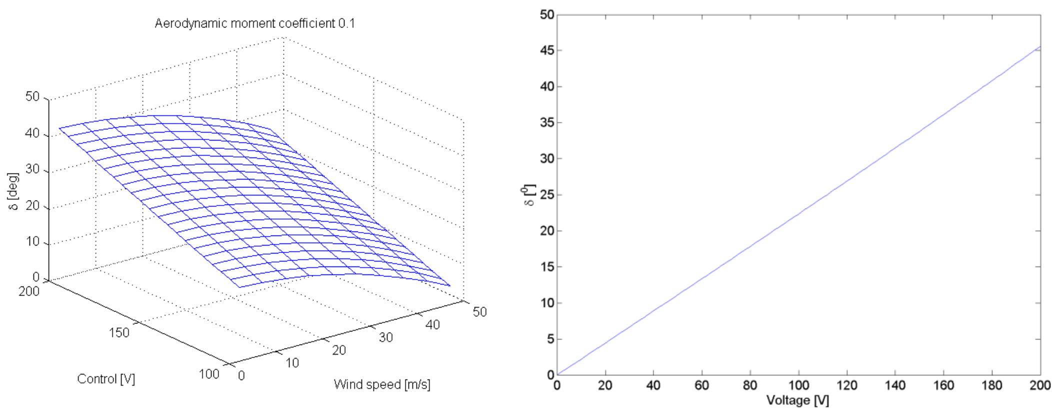

Figure 6. Left: stationary values of the angle δ, developed by piezostack actuator, in the presence of the load F_a; right: evolution of the aileron deflection angle (Fig. 5) with respect to the voltage V

c) in the presence of the control voltage *V*, the piezo stack P_1P_3 develops an expansion movement, and the piezo stack P_2P_4 develops a movement of withdrawal, if it has previously been extended, and, based on constraints, the point P_3 moves on an arc in the point P'_3, the lever P'_3M' remaining solidary, without deformations, with P_0M'.

The results of the numerical simulations of the piezo actuator, in correlation with the lab measurements, are given in Figure 6. These confirm that the actuator was designed and manufactured in accordance with the strict requirements imposed by the control law implemented for the tests in aerodynamic tunnel.

4 MODAL TESTS ON AFDPA SYSTEM

The elastic wing was designed as a scale model of a real wing, in contrast to the rigid models presented in the literature where the elasticity is simulated through external springs. Other objective taken into account during the design phase of the wing was to ensure the flutter of the uncontrolled system given the conditions of the subsonic tunnel from INCAS.
The flutter induction experiment led to the following results, important for the entire project: **flutter speed: 41 m/s, flutter frequency: 5.8 Hz**. As it was expected, the structure of the wing, exactly the longeron, suffered major damages during the flutter, therefore a new specimen had to be manufactured. The designer of the new specimen had to provide a wing with a lighter aileron meeting the requirements of the first two frequencies determined by the designer of the damaged wing, eng. V. Turcan (CATIA estimation **6.23** and **10.21 Hz)** and measured (**5.93** and **11.58 Hz** for the wing with simulated actuator mass and with two gripping screws for wood elements).
From the analysis of the recorded film during the flutter experiment it was possible to observe the torsion of the model, visible also in Fig. 7. Flutter vibration is, however, more complex, overlapping the bending and torsion of the first two elementary modes. The challenge that starts from here is to find a suitable topography for sensors (accelerometers) placements, see Fig. 7 right.

Figure 7: Left: the wing model mounted for the flutter experiment in the subsonic tunnel; middle: the sequence of flutter evolution of the wing at air speed of 41 m/s; right: the scheme of accelerometers placements on the wing model

The natural frequencies of the AFDPA wing were experimentally determined in two configurations:

- The AFDPA wing was tried in its initial configuration - with all the fastening screws of the wooden elements
- The AFDPA wing was tried in a less rigid configuration – 4 screws were removed (fastening screws of the wooden elements - 2 on intrados, 2 on extrados). In this configuration all the wooden elements are mounted on the resistance structure only by 2 screws, one on intrados and one on extrados.

There is a slight decrease in the torsion frequency for the less rigid configuration (type 2 configuration - without screws). The processed data are presented for two representative tests (type 1 configuration and type 2 configuration) in the graphs below. The values measured at STRAERO for sample no. 1, (5.93 and 11.58 Hz, for wing with simulated mass of the actuator and with 2 fastening screws on the wooden elements), are reproduced on sample no. 2.

Table 1: Important natural frequencies for flutter

Natural frequencies	Type 1 configuration	Type 2 configuration
First bending frequency	6.37 Hz	6.37 Hz
First torsion frequency	16.63 Hz	14.94 Hz

5 FUNCTIONAL AND PERFORMANCE TESTS WITH THE ACTUATOR

The important result of the functional tests with the integrated actuator on the wing (Figure 8) is that an internal PID loop ensures the stability of the movement and a bandwidth of about 20 Hz (Figure 9, green curves). It is estimated that the frequency of 20 Hz is consistent in the context in which the actuator is supposed to suppress an identified frequency of the 5.8 Hz flutter.

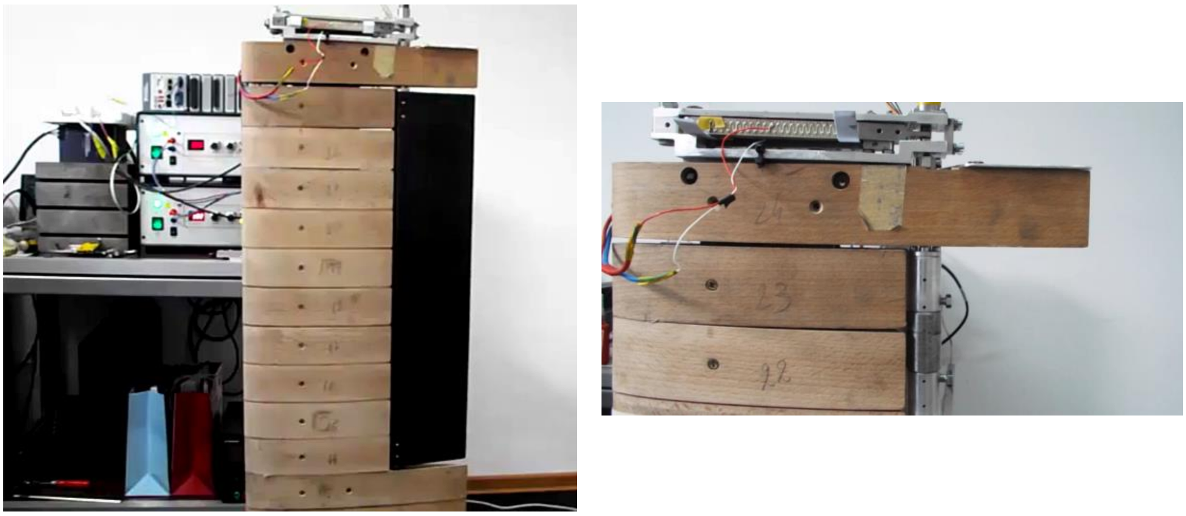

Figure 8: left: tests on the wing with aileron; right: tests on the wing with equivalent mass

6 CONTROL SYNTHESIS AND IMPLEMENTATION BY RECEPTANCE METHOD

The antiflutter control algorithm based on the receptance method [3] involves identifying the model simultaneously with determining the amplifications in the response loops from the distributed sensors on the model. In this case, the identification of the experimental model requires a more accurate acquisition of the resonance frequencies of the system in the open loop. Resonant frequencies are identified by generating sample signals using a function generator connected via a USB port to a computer. This sample signal, amplified with a high voltage amplifier, is directed to the piezo actuator. The response signal of the structure is picked up by two accelerometers and processed by the B&K preamplifier. From the preamplifier, the signal is took over by an oscilloscope connected via the USB port to the same computer. Both chirp and impulse signals were generated. Practically, the methodology involves on-line measurements of the frequency response, eluding the need for knowing the matrix **M, C, K** (mass, damping, stiffness matrices) and **b** (influence vector). It is not necessary either to reduce the order of the model or to synthesize an estimator for the unmeasured state. In principle, this controller can be continuously corrected on the basis of measurements, with beneficial consequences in increasing the manoeuvrability and reducing the risk of flutter.
The method for a single input control is briefly given. The second order matrix equation is

$$\left(\mathbf{M}s^2+\mathbf{C}s+\mathbf{K}\right)\mathbf{x}(s)=\mathbf{b}(s)u(s)+\mathbf{p}(s) \tag{2}$$

where **u** represents the control, and **p**(s) is an external perturbation. The influence vector (through which the control is located), **b**(s), is written as a function of s. An usual form is that of PI (proportional-integral)

$$u(s) = -\begin{pmatrix}\mathbf{f}^{T} & \mathbf{g}^{T}\end{pmatrix}\begin{pmatrix} s\mathbf{x} \\ \mathbf{x}\end{pmatrix} = -(s\mathbf{f}+\mathbf{g})^{T}\mathbf{x} \tag{3}$$

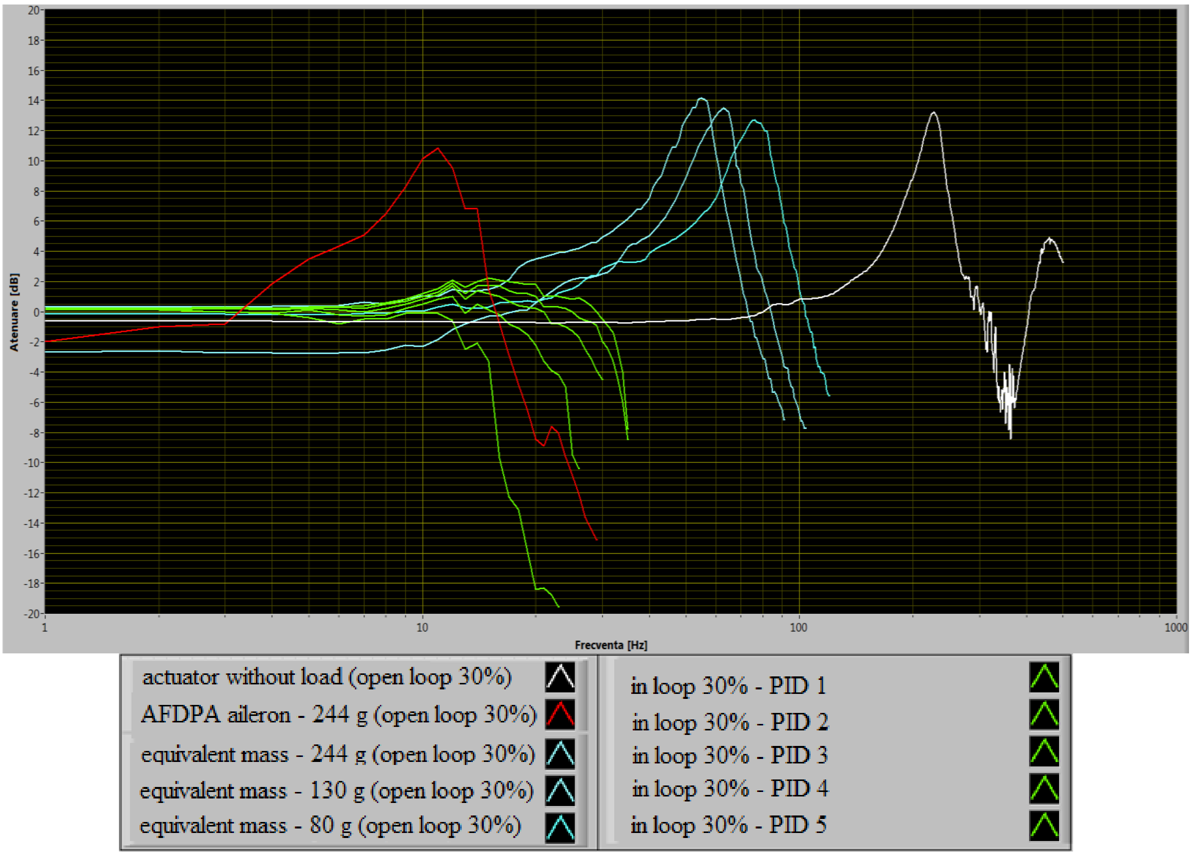

Figure 9: Frequency characteristics of the actuator

$$\mathbf{b}(s) = \mathbf{b}_1 + \frac{\mathbf{b}_2}{s} \tag{4}$$

It results from (2) and (3)

$$\left(\mathbf{M}s^2 + \left(\mathbf{C} + \mathbf{b}(s)\mathbf{f}^{T}\right)s + \left(\mathbf{K} + \mathbf{b}(s)\mathbf{g}^{T}\right)\right)\mathbf{x}(s) = \mathbf{p}(s) \tag{5}$$

with the consequence of changing the stiffness matrix rank. The Sherman-Morrison formula reverses a matrix in the case of the change of rank depending on the inverse of the original matrix

$$\hat{\mathbf{H}}(s) = \mathbf{H}(s) - \frac{\mathbf{H}(s)\mathbf{b}(s)(\mathbf{g}+s\mathbf{f})^{T}\mathbf{H}(s)}{1+(\mathbf{g}+s\mathbf{f})^{T}\mathbf{H}(s)\mathbf{b}(s)} \tag{6}$$

Where

$$\mathbf{H}(s) = \left(\mathbf{M}s^2 + \mathbf{C}s + \mathbf{K}\right)^{-1} \tag{7}$$

The characteristic polynomial of the closed loop system is $1+(\mathbf{g}+s\mathbf{f})^{T}\mathbf{H}(s)\mathbf{b}(s)$ and the issue of allocating the poles of the system to the values $\{\mu_1 \quad \mu_2 \quad \mathrm{K} \quad \mu_{2n}\}$ can be solved as shown below. If we note

$$\mathbf{r}_k(\mu_k) = \mathbf{H}(\mu_k)\mathbf{b}(\mu_k) \tag{8}$$

then, for the characteristic equation, we have

$$\mathbf{r}_k^{T}(\mu_k)\times(\mathbf{g}+\mu_k\mathbf{f}) = -1,\ k=1,\mathrm{K}\ ,2n \text{ or } \mathbf{r}_k^{T}\mathbf{g}+\mu_k\mathbf{r}_k^{T}\mathbf{f} = -1,\ k=1,\mathrm{K}\ ,2n \tag{9}$$

The set of 2n equations with 2n unknown can be written in matrix form

$$\mathbf{G}\begin{pmatrix}\mathbf{g}\\ \mathbf{f}\end{pmatrix}=\begin{pmatrix}-1\\ -1\\ \vdots\\ -1\end{pmatrix},\quad \mathbf{G}=\begin{bmatrix}\mathbf{r}_1^T & \mu_1\mathbf{r}_1^T\\ \mathbf{r}_2^T & \mu_2\mathbf{r}_2^T\\ \vdots & \vdots\\ \mathbf{r}_{2n}^T & \mu_{2n}\mathbf{r}_{2n}^T\end{bmatrix} \qquad (10)$$

allowing, thus, the determination of **g** and **f** by inversion of the matrix. Relationship (10) is essential in the synthesis of control by the receptance method.

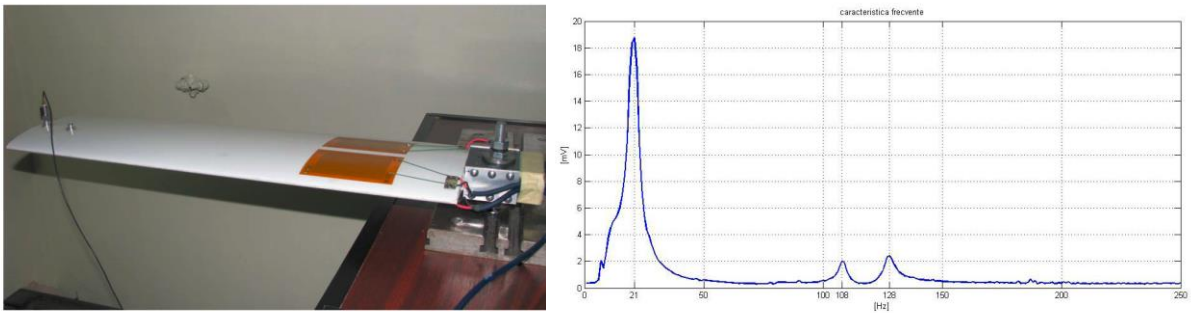

Figure 10: left: Hardware wing model for testing the synthesis algorithm of the control by the receptance method; b) the first three resonance frequencies

The receptance method was tested "on the ground" in the INCAS Mechatronics Laboratory on the model shown in Figure 10. The eloquent results are shown in Figure 11.

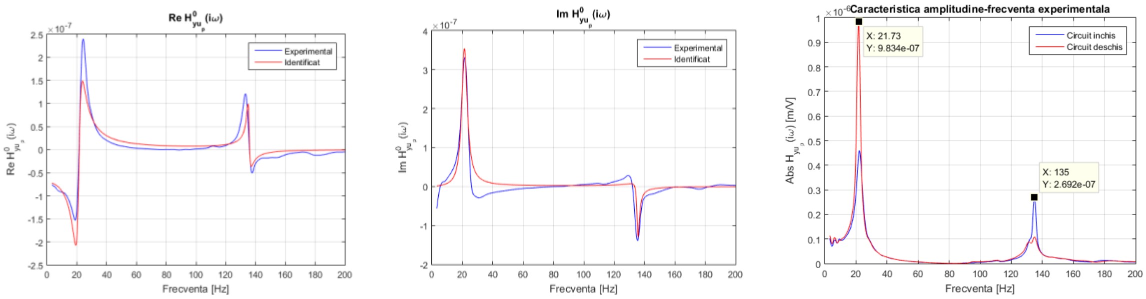

Figure 11: Testing the receptance method on the model from Figure 10: left and middle: the identification of the excitator (piezo actuator)-transducer function is accurate; right: the resonances of the system are well amortized in the loop

Figure 12: AFDPA system tested in INCAS subsonic tunnel

The AFDPA system is currently being validated in the aerodynamic tunnel (Figure 12). One can see the position of the two accelerometers at the top of the wing. The first results show that the receptance method works in the sense that the identification of the transfer functions is relevant, leading to the synthesis of control according to the relationship (10). The tests were already done at a speed of 30 m/s. The project ends in late September. The next step is to validate the system by exceeding the flutter speed set in the earlier stages of the project.

7 CONCLUDING REMARKS

INCAS Mechatronics Laboratory has a tradition of over 45 years in analysis, synthesis, qualified testing and flight clearance for aircraft and helicopters hydraulic servomechanisms [4]. More recent is research on smart structures [5]-[12]. Successful completion of the project opens up perspectives for further research in the field. We mention that a similar research is present in laboratories in England [13], but we do not know how it was completed.

ACNOWLEDGEMENTS

The authors gratefully acknowledge the financial support of the National Authority for Scientific Research–ANCS, UEFISCSU, through AFDPA research project Contract 289/2014.

REFERENCES

[1] * * * *Antiflutter demonstrator with piezoelectric actuator*, PN-II-PT-PCCA-2013-4-2006, Contract 289/2014

[2] Ursu, I., Ion Guta, D. D., Enciu, D., Toader, A., Dan, M., Donciu, C., Turcan, V.; 2016; "Mathematical modeling of a V-stack piezoelectric aileron actuation"; *INCAS Bulletin*; **8**; (4); 141-155

[3] Ram, Y. M., Mottershead, J. E.; 2007; "Receptance method in active vibration control"; *American Institute of Aeronautics and Astronautics Journal*; **45**; (3); 562-567

[4] Ursu, I., Ursu, F.; 2002; *Active and semiactive control* (in Romanian); Publishing House of the Romanian Academy; Bucharest; ISBN 973-27-0894-8

[5] Ursu, I.; Stoia-Djeska, M., Ursu, F.; 2004; "Active control laws for flutter suppression"; *Annales of University of Craiova, Electrical Engineering Series*; **27;** (27), 62-70

[6] Ursu, I., Iorga, L., Toader, A., Tecuceanu, G.; 2011; "Active Robust Control of a Smart Plate"; *ICINCO 2011 8th International Conference on Informatics in Control, Automation and Robotics*; Noordwijkerhout; The Netherlands; 28-31 July 2011

[7] Ursu, I., Enciu, D., Toader, A.; 2016; "Towards structural health monitoring of space vehicles"; *Aircraft Engineering and Aerospace Technology*; DOI: 10.1108/AEAT-07-2015-0173.R1. hard publication 2017

[8] Iorga, L., Baruh, H., Ursu, I.; 2009; " H_∞ control with μ-analysis of a piezoelectric actuated plate; *Journal of Vibration and Control*; 15; (8); 1143-1171

[9] Iorga, L., Baruh, H., Ursu I.; 2008; "A review of H_∞ robust control of piezoelectric smart structures", *Transactions of the ASME*, *Applied Mechanics Reviews*; 61**;** (4); 17-31

[10] Enciu Daniela, I. Ursu, A. Toader (2016-2017), "New Results Concerning SHM Technology Qualification for Transfer on Space Vehicles", in press in *Structural Control and Health Monitoring, 2017,* 2017;e1992. https://doi.org/10.1002/stc.1992

[11] Ursu, I., Daniela Enciu, A. Toader (2016), Towards structural health monitoring of space vehicles, *Aircraft Engineering and Aerospace Technology*, DOI: 10.1108/AEAT-07-2015-0173.R1. hard publication 2017

[12] Enciu Daniela, I. Ursu, M. Tudose; 2016; "Towards Space applications of SHM technology relied on EMIS method", *Proc. of EWSHM 2016*, vol. 21, no. 8, ISSN 1435-4934, 2016

[13] Papatheou, E., Tantaroudas, N. D., Da Ronch, A., Cooper, J. E. and Mottershead, J. E.; 2013; "Active control for flutter suppression: an experimental investigation"; At *International Forum on Aeroelasticity and Structural Dynamics (IFASD),* United Kingdom; 24 - 27 Jun 2013